PHYSICAL REVIEW D VOLUME 32, NUMBER 7 1 OCTOBER 1985

Role of the QCD-induced gluon-gluon coupling to gauge-boson pairs in the multi-TeV region

Ll. Ametller*
International Centre for Theoretical Physics, Trieste, Italy

E. Gava
Istituto Nazionale di Fisica Nucleare, Sezione di Trieste, Trieste, Italy

N. Paver and D. Treleani
Dipartimento di Fisica Teorica, Università di Trieste, Trieste, Italy
and Istituto Nazionale di Fisica Nucleare, Sezione di Trieste, Trieste, Italy

(Received 25 March 1985; revised manuscript received 28 June 1985)

We discuss the production of $\gamma\gamma$ and $Z^0\gamma$ pairs induced by the gluon-gluon fusion mechanism at typical supercollider energies. Due to the large flux of gluons with small fractional momenta, it is found that in certain kinematical configurations this subprocess, although of order $(\alpha_s/\pi)^2$ with respect to the leading quark annihilation, can give an appreciable contribution to the cross section for $Z^0\gamma$ production and even a larger one for the $\gamma\gamma$ production.

I. INTRODUCTION

Hadronic production of intermediate-vector-boson pairs will be extensively studied at the future supercolliding $p\bar{p}$ machines.[1] At the leading order in QCD and in the electroweak coupling constant the dominant process is represented by the quark-antiquark annihilation. The typical values of the partons fractional momenta which are relevant to boson pair production are of order $x \sim M_Z/E_{\rm c.m.}$ and can therefore be as small as 10^{-3}—10^{-2} for center-of-mass energies of 10—40 TeV. In such a small x range the number of gluons in the colliding p and $\bar{p}$ becomes much larger than that of quarks and antiquarks.[2] Due to this increased gluon luminosity, one can expect that gluon-gluon-initiated processes in the hard interaction (although of higher order in α_S) can play a role with respect to the leading, quark-induced ones. In this context it should be interesting to analyze the contribution of the gluon-fusion process represented by the quark box diagram of Fig. 1 (and crossed ones). Compared to the $q\bar{q}$ annihilation this process contributes an order $(\alpha_S/\pi)^2$ to the cross section. In the expansion of the latter in powers of α_S there are, of course, many other terms, proportional to α_S and to $\alpha_S{}^2$, which originate from QCD corrections to the quark-antiquark annihilation and also from quark-gluon-induced processes, and which are known only to a limited extent. Among other things, these corrections affect the leading QCD definition of the Q^2-dependent quark and gluon distributions. From this point of view, the quark box in Fig. 1 is thus one among the corrections of $O(\alpha_S{}^2)$. Nevertheless, as it contributes positively to the cross section and can be consistently estimated by using the gluon distributions at the leading order in QCD without requiring the knowledge of the other corrections mentioned above, it represents as it stands a well-defined term which is sensible to analyze.

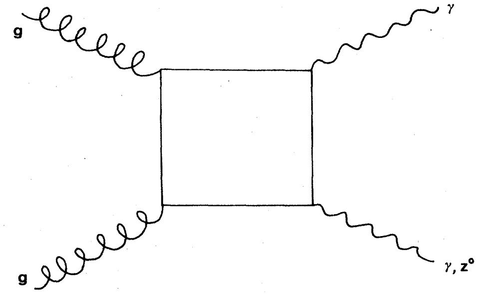

FIG. 1. Quark loop diagram for the gg-induced production of $\gamma\gamma$ and $Z^0\gamma$ pairs.

The $\gamma\gamma\to\gamma\gamma$ scattering via the fermion box diagram is a classical issue in the context of QED, and has received much attention in the past.[3,4] The calculation of the box diagram in the general configuration is a very complicated technical problem, and leads to cumbersome formulas, which have been explicitly worked out, for off-shell final photons, in Ref. 4. Thus, in the present paper we will utilize the results of Ref. 4 in order to discuss, as the simplest applications, the cases of $gg\to\gamma\gamma$ and $gg\to Z^0\gamma$. Although rather special at first sight, these processes should already be representative (at least in a qualitative sense) of the role of the gluon-gluon box diagram in the more general case of the production of two massive bosons at the supercolliders. For $gg\to\gamma\gamma$ relatively simple formulas can be written down which, however, have only been exploited so far at the lower energy of present colliders.[5] For $gg\to Z^0\gamma$ such a compact formulation does not exist. In the next section we will briefly describe the procedure followed to derive the $gg\to Z^0\gamma$ helicity amplitudes, as well as the various inputs used in order to compute the $\gamma\gamma$ and $Z^0\gamma$ production cross sections in $p\bar{p}$. In

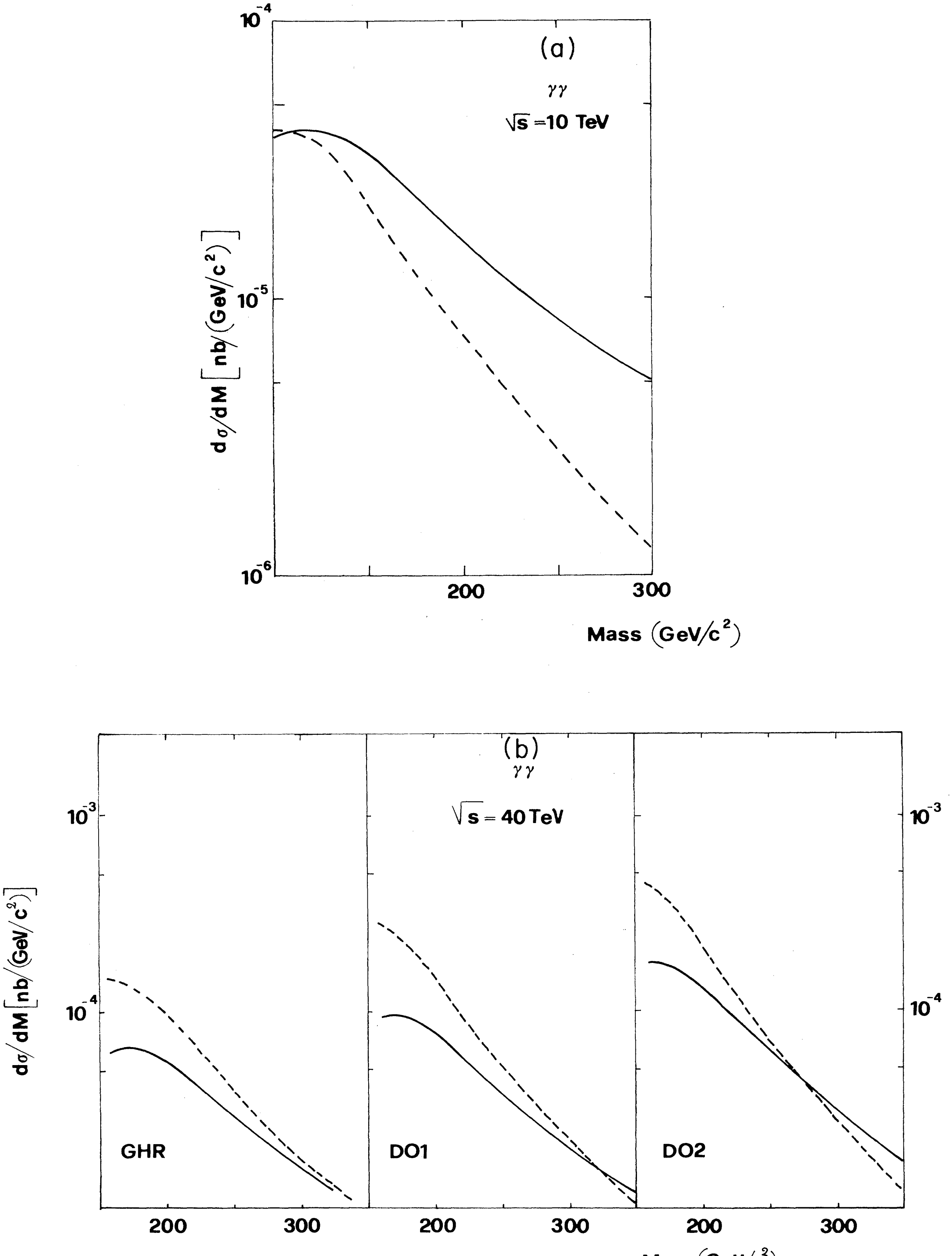

FIG. 2. Mass spectrum of $\gamma\gamma$ pairs produced in $p\bar{p}$ collisions at $\sqrt{s}=10$ TeV (a) and $\sqrt{s}=40$ TeV (b). Solid curve, $q\bar{q}$ annihilation; dashed curve, gg-initiated process. The allowed minimum transverse momentum for the photons is 50 GeV/c. The rapidity cut Y is 2.5.

the last section a discussion is given of the results so obtained.

II. CALCULATIONS

First of all, the gluons in Fig. 1 can be formally replaced by photons, with $\alpha \to \alpha_S$ and a color factor $\frac{1}{4}\mathrm{Tr}\lambda^a\lambda^b$. Second, the $\gamma_\mu\gamma_5$ coupling of the Z^0 to quarks should not contribute by C parity, so that only the vector coupling of the Z^0,

$$\gamma_\mu \frac{1}{i\sqrt{2}}\left[\frac{G_F M_Z{}^2}{\sqrt{2}}\right]^{1/2}(\tau_3 - 4e_q \sin^2\theta_W) ,$$

is active. Finally, there is the quark electric charge ee_q at the photon vertex. With these replacements one can use the expressions for the box four-point function $G_{\mu\nu\rho\sigma}$ given in Ref. 4 for the case of one nonvanishing and spacelike external mass. Formulas are presented in Ref. 4 in a form which allows a straightforward continuation to timelike external masses. The amplitude for $gg \to Z^0\gamma$ is finally obtained by summing the coherent contributions of all quark species. At the high energies we are interested in, it should be a safe approximation to neglect the masses of the u, d, s, c, and b quarks. In this $m_q = 0$ limit the various $gg \to Z^0\gamma$ helicity amplitudes, although quite complicated by the presence of $M_Z \neq 0$, are still manageable, and we report them explicitly in the Appendix. One can notice that, compared to the case of the $\gamma\gamma$ final state, there are eight independent transverse amplitudes instead of five, essentially due to the nonidentity of γ and Z^0. There are, in addition, four independent longitudinal amplitudes, which are easily derived by defining the appropriate Z^0 longitudinal polarization vector and utilizing the relations given in Ref. 4. As regards the top quark we should in principle retain m_t and use the full mass-dependent formulas which, however, become quite unwieldy and no longer expressible in terms of Spence functions with real arguments. On the other hand, such a calculation should not be so important in practice in the regime we are interested in, as we can expect, rather generally, that the top-quark box diagram should be depressed by the large m_t, so that the ultimate result should be determined almost entirely by the box diagrams with just the "massless" u, d, s, c, and b quarks.[6(a)] Accordingly, we have disregarded the top quark in our calculation. While this should be a very reasonable approximation for the $\gamma\gamma$ case, the depression due to m_t could be much less severe in the $Z^0\gamma$ case.[6(b)] On the other hand, taking rigorously into account such an effect here would certainly affect the final result for the cross section much less than the other overall uncertainties (e.g., those due to the parton distributions) which are present in the calculation.

The amplitude for the process $gg \to \gamma\gamma$ can be directly obtained from the Appendix by taking the limit $M_Z \to 0$ and by suitably redefining the coupling constant. We have explicitly checked that one reobtains in this way the amplitudes given in Ref. 5.

The differential cross section for $gg \to Z^0\gamma$ averaged over the color and the spin of the gluons reads

$$\frac{d\sigma}{dz}(gg \to Z\gamma) = \frac{\alpha_{\mathrm{em}}{}^2}{16\pi}\frac{\alpha_s{}^2}{\hat{s}}\left[\sum_{\mathrm{quarks}} \frac{e_q(\tau_3 - 4e_q\sin^2\theta_W)}{4\sin\theta_W\cos\theta_W}\right]^2 \times \left[1 - \frac{M_Z{}^2}{\hat{s}}\right]\frac{1}{4}\sum_{i=1}^{24}|M_i|^2 , \tag{1}$$

where $\hat{s}$ and $z = \cos\theta$ represent, respectively, the parton c.m.-frame energy squared and scattering angle, and the M_i are the helicity amplitudes explicitly given in the Appendix. A significant observable is the cross section to produce a $Z\gamma$ (or a $\gamma\gamma$) pair of invariant mass $M = \sqrt{\tau s}$, where $\sqrt{s}$ is the colliding $p\bar{p}$ c.m.-frame energy, with both bosons in a rapidity interval (in that frame) $-Y < y < Y$. One has

$$\frac{d\sigma}{dM}(p\bar{p} \to Z^0\gamma + \text{anything}) = \frac{2M}{s}\int_{-Y}^{Y} dy_{\mathrm{boost}}\, G_p(x_a, M_Z{}^2) \times G_{\bar{p}}(x_b, M_Z{}^2)\int_{z_1}^{z_2} dz \frac{d\sigma}{dz}(gg \to Z^0\gamma) , \tag{2}$$

where $G(x,Q^2)$ is the gluon fractional momentum distributions, and

$$y_{\mathrm{boost}} = \tfrac{1}{2}\ln(x_a/x_b)$$

relates the gg c.m. frame to the $p\bar{p}$ c.m. frame, such that

$$\begin{aligned} x_a &= \sqrt{\tau}e^{y_{\mathrm{boost}}} , \\ x_b &= \sqrt{\tau}e^{-y_{\mathrm{boost}}} , \end{aligned} \tag{3}$$

and the angular-integration limits z_1, z_2 are determined by Y and by the requirement that the photon has a minimum $p_\perp$. As there is no well-defined prescription for the process under consideration, we have indicatively chosen as the "large" scale in α_S and in the partons distributions $Q^2 = M_Z{}^2$. The parton distributions used in the calculation are those of Ref. 7(a) (GHR) with a value $\Lambda = 0.4$ GeV, and both the set 1 and the set 2 distributions of Ref. 7(b) (DO1 and DO2) with $\Lambda = 0.2$ and 0.4 GeV, respectively.

We have computed Eq. (2) versus M for $p\bar{p}$ c.m. energies of 10 and 40 TeV, with a minimum $p_\perp$ of the photon of 50 GeV and $Y = 2.5$. The results are shown in Figs. 2(a), 2(b), 3(a), and 3(b) and compared to the leading-order $q\bar{q}$ annihilation for the production of $\gamma\gamma$ and $Z^0\gamma$, respectively. The results at $\sqrt{s} = 10$ TeV are rather insensitive to the input parton distributions, so that in Figs. 2(a) and 3(a) we represent by just one curve the three cases considered. On the contrary, the dependence on the parton distributions turns out to be much more significant at $\sqrt{s} = 40$ TeV, due to the smaller values of x involved, and is explicitly displayed in Figs. 2(b) and 3(b).

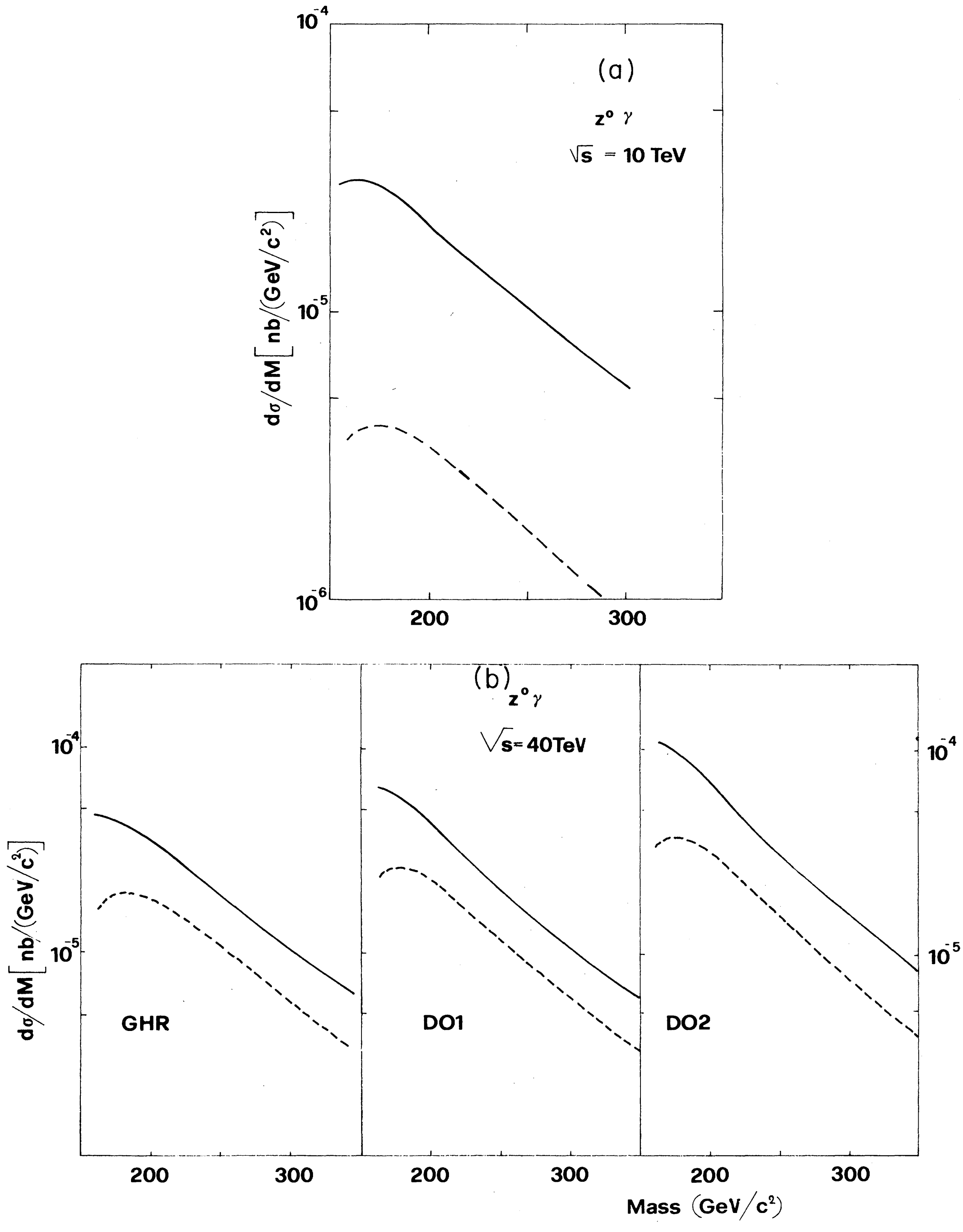

FIG. 3. Same as Fig. 2 for the $Z^0\gamma$ mass spectrum. The allowed minimum transverse momentum for the photon is 50 GeV/c. The rapidity cut Y is 2.5.

III. DISCUSSION

As one can see from the figures, the contribution of the box diagram for $Z^0\gamma$ is a correction to the leading mechanism at $\sqrt{s}=10$ TeV. At the larger value $\sqrt{s}=40$ TeV it increases, however, appreciably, to the point of reaching roughly the same size as the $q\bar{q}$-induced cross section. In the case of $\gamma\gamma$ production the contribution of the box diagram is already of the same size of the annihilation diagram at $\sqrt{s}=10$ TeV and can be even a factor of 2 or 3 larger, in the peak region, at $\sqrt{s}=40$ TeV. This is due to the combined effect of the increase of the gluon flux with respect to the quark flux for smaller values of the partons fractional momenta x_a, x_b and to the rapidity cuts which constrain the integration region in Eq. (2) away from the forward direction and accordingly reduce the importance of the t pole in the $q\bar{q}$ annihilation diagram. For the latter reason one can see that if the value of the rapidity cutoff Y is decreased by some factor, the ratio of the box to the $q\bar{q}$ cross sections proportionally increases. All of these effects are such that the $(\alpha_S/\pi)^2$ factor of the box diagram relative to the $q\bar{q}$ annihilation is largely recovered.

One can also remark that the box diagram produces a smaller effect in the case of $Z^0\gamma$, compared to the case of $\gamma\gamma$ (of course, within the same cuts). This is due to some extent to $M_Z \neq 0$, but also in large part to the explicit value of the electroweak couplings of the Z^0 to quarks. We should also point out that although, as expected, the cross sections depend rather sensitively on the chosen cut on the minimal $p_\perp$ of the photon, the relative importance of the box and the $q\bar{q}$ does not appear to change qualitatively.

The cuts in the rapidity and in $p_\perp$ imposed in our explicit calculation are in line with the criterion suggested in Ref. 1. The resulting cross sections both of the $q\bar{q}$- and of the gg-induced $\gamma\gamma$ and $Z^0\gamma$ production processes are rather small. However, owing to, the large luminosity which is expected to be achieved at the superconducting supercollider, they should be well within the limits of observability.

On the basis of the results described above for the simplest case of $\gamma\gamma$ and $Z^0\gamma$, we can expect a similar trend for the more general (and more complicated) case of ZZ and WW production.

ACKNOWLEDGMENTS

Fruitful discussions with Professor G. Altarelli are gratefully acknowledged. We also thank Dr. M. Samuel for a useful correspondence. One of us (Ll.A.) would like to thank Professor Abdus Salam, the International Atomic Energy Agency and UNESCO for hospitality at the International Center for Theoretical Physics, Trieste.

APPENDIX

Here we give the expression for the 24 helicity amplitudes contributing to the process $Z\gamma \to gg$. For any helicity amplitude M_{ijkl}, the first index refers to the polarization state of the Z boson and the second, third, and fourth to the photon, gluon, and gluon helicity states, respectively:

$$M_{+-+-}(s,t,u)=M_{-+-+}(s,t,u)=\frac{1}{2}\left[\frac{s+M_Z{}^2}{s_1}\frac{E_+^{(1)}(u,t,s)}{8u_1}+\frac{E_+^{(1)}(u,s,t)}{8u_1}\right]+\frac{E_+^{(2)}(u,t,s)}{8}, \tag{A1}$$

$$M_{++--}(s,t,u)=M_{--++}(s,t,u)=-\frac{1}{2}\left[\frac{E_-^{(1)}(s,t,u)}{8s_1}+\frac{E_-^{(1)}(s,u,t)}{8s_1}\right]+\frac{E_-^{(2)}(s,t,u)}{8}, \tag{A2}$$

$$M_{++++}(s,t,u)=M_{----}(s,t,u)=\frac{1}{2}\left[\frac{E_+^{(1)}(s,t,u)}{8s_1}+\frac{E_+^{(1)}(s,u,t)}{8s_1}\right]+\frac{E_+^{(2)}(s,t,u)}{8}, \tag{A3}$$

$$M_{+--+}(s,t,u)=M_{-++-}(s,t,u)=\frac{1}{2}\left[\frac{E_+^{(1)}(t,s,u)}{8t_1}+\frac{s+M_Z{}^2}{s_1}\frac{E_+^{(1)}(t,u,s)}{8t_1}\right]+\frac{E_+^{(2)}(t,s,u)}{8}, \tag{A4}$$

$$M_{+++-}(s,t,u)=M_{---+}(s,t,u)=-\frac{1}{2}\left[\frac{E_+^{(1)}(t,s,u,)}{8t_1}+\frac{s+M_Z{}^2}{s_1}\frac{E_+^{(1)}(t,u,s)}{8t_1}\right]+\frac{E_+^{(2)}(t,s,u)}{8}, \tag{A5}$$

$$M_{++-+}(s,t,u)=M_{--+-}(s,t,u)=-\frac{1}{2}\left[\frac{s+M_Z{}^2}{s_1}\frac{E_+^{(1)}(u,t,s)}{8u_1}+\frac{E_+^{(1)}(u,s,t)}{8u_1}\right]+\frac{E_+^{(2)}(u,t,s)}{8}, \tag{A6}$$

$$M_{+-++}(s,t,u)=M_{-+--}(s,t,u)=\frac{1}{2}\left[\frac{E_-^{(1)}(s,t,u)}{8s_1}+\frac{E_-^{(1)}(s,u,t)}{8s_1}\right]+\frac{E_-^{(2)}(s,t,u)}{8}, \tag{A7}$$

$$M_{-+++}(s,t,u)=M_{+---}(s,t,u)=-\frac{1}{2}\left[\frac{E_+^{(1)}(s,t,u)}{8s_1}+\frac{E_+^{(1)}(s,u,t)}{8s_1}\right]+\frac{E_+^{(2)}(s,t,u)}{8}, \tag{A8}$$

$$M_{0+++}(s,t,u)=-M_{0---}(s,t,u)=\left[\frac{-M_Z{}^2}{2stu}\right]^{1/2}\left[t\frac{E_+^{(1)}(s,u,t)}{8s_1}-u\frac{E_+^{(1)}(s,t,u)}{8s_1}\right], \tag{A9}$$

$$M_{0-++}(s,t,u)=-M_{0+--}(s,t,u)=\left[\frac{-M_Z{}^2}{2stu}\right]^{1/2}\left[t\frac{E_-^{(1)}(s,u,t)}{8s_1}-u\frac{E_-^{(1)}(s,t,u)}{8s_1}\right], \tag{A10}$$

$$M_{0+-+}(s,t,u)=-M_{0-+-}(s,t,u)=-\left[\frac{-M_Z^2}{2stu}\right]^{1/2}\left[t\frac{E_+^{(1)}(u,s,t)}{8u_1}+\frac{s(t-u)}{s_1}\frac{E_+^{(1)}(u,t,s)}{8u_1}\right], \tag{A11}$$

$$M_{0++-}(s,t,u)=-M_{0--+}(s,t,u)=\left[\frac{-M_Z^2}{2stu}\right]^{1/2}\left[u\frac{E_+^{(1)}(t,s,u)}{8t_1}-\frac{s(t-u)}{s_1}\frac{E_+^{(1)}(t,u,s)}{8t_1}\right]. \tag{A12}$$

$M_Z{}^2$ is the Z-boson mass squared, s, t, u are the Mandelstam variables satisfying

$$s+t+u=M_Z{}^2 ,$$

and the notation $x_1=x-M_Z{}^2$ is used. The functions $E_+^{(i)}(x,y,z)$ and $E_-^{(i)}(x,y,z)$ correspond to $E_{+++}^{(i)}(jklm)$ and $E_{-++}^{(i)}(jklm)$ in Ref. 4 in an obvious correspondence among respective arguments [i.e., $E_+^{(i)}(s,t,u)=E_{+++}^{(i)}(1234)$, $E_-^{(i)}(t,s,u)=E_{-++}^{(i)}(1324)$, and so on].

Equations (A1)–(A12) as they stand are valid for any value of the quark mass m. However, we worked out the zero quark mass limit and in this particular case the functions $E_\pm^{(i)}(x,y,z)$ simplify considerably. They explicitly read

$$\frac{E_+^{(1)}(x,y,z)}{8x_1}=\frac{2y}{x_1}\left[\frac{-z}{y_1}+\frac{z}{x}\left[2-\frac{x}{z_1}\right]G(z,y)+\frac{M_Z{}^2}{y_1}\left[\frac{2z}{x}-\frac{2z}{y_1}+\frac{y_1}{z_1}-1\right]G(M_Z{}^2,y)+\frac{y}{x}\left[1-\frac{z}{y}-\frac{2z}{x}\right]H(y,z,-M_Z{}^2)\right], \tag{A13a}$$

$$\frac{E_+^{(2)}(x,y,z)}{8}=\left[\frac{z}{x}\left[2+\frac{x}{z_1}\right]G(z,y)-\frac{M_Z{}^2}{x}\left[2+\frac{x}{y_1}+\frac{x}{z_1}\right]G(M_Z{}^2,y)+\frac{x_1}{x}\left[1-\frac{2yz}{x_1x}\right]H(y,z,-M_Z{}^2)\right], \tag{A13b}$$

$$E_-^{(1)}(x,y,z)=0\ ,\quad \frac{E_-^{(2)}(x,y,z)}{8}=-1\ . \tag{A13c}$$

The functions $G(x,y)$ and $H(x,y,-M_Z{}^2)$ are defined as

$$G(x,y)=-G(y,x)\ , \tag{A14a}$$

$$\mathrm{Re}\,G(x,y)=\tfrac{1}{2}\ln\left|\frac{x}{y}\right| , \tag{A14b}$$

$$\mathrm{Im}\,G(x,y)=-\frac{\pi}{2}[\theta(x)-\theta(y)]\ , \tag{A14c}$$

$$H(x,y,-M_Z{}^2)=H(y,x,-M_Z{}^2)\ , \tag{A15a}$$

$$\begin{aligned}\mathrm{Re}\,H(x,y,-M_Z{}^2)=-\frac{1}{4}\Bigg\{&-2\,\mathrm{Re}\,\mathrm{Li}_2\left[\frac{zM_Z{}^2}{zM_Z{}^2+xy}\right]+2\,\mathrm{Re}\,\mathrm{Li}_2\left[\frac{z}{y+z}\right]+2\,\mathrm{Re}\,\mathrm{Li}_2\left[\frac{z}{z+x}\right]\\&+\mathrm{Re}\ln^2\left[\frac{z+y}{y}\right]+\mathrm{Re}\ln^2\left[\frac{z+x}{x}\right]-\mathrm{Re}\ln^2\left[\frac{zM_Z{}^2+xy}{xy}\right]\\&-2\,\mathrm{Re}\left[\ln\left[\frac{z+y}{y}\right]\ln\left[\frac{x}{M_Z{}^2}\right]\right]-2\,\mathrm{Re}\left[\ln\left[\frac{z+x}{x}\right]\ln\left[\frac{y}{M_Z{}^2}\right]\right]\Bigg\},\end{aligned} \tag{A15b}$$

$$\mathrm{Im}\,H(x,y,-M_Z{}^2)=-\frac{\pi}{2}\left[\ln\left|\frac{y+z}{y}\right|\theta(x)+\ln\left|\frac{x+z}{x}\right|\theta(y)+\ln\left|\frac{xy}{xy+zM_Z{}^2}\right|\theta(M_Z{}^2)\right]. \tag{A15c}$$

In Eqs. (A15b) and (A15c) $z=-(x+y-M_Z{}^2)$, and the dilogarithm is defined as usual

$$\mathrm{Li}_2(x)=-\int_0^x\frac{\ln(1-t)}{t}dt\ . \tag{A16}$$

The amplitudes for $\gamma\gamma\to gg$ transition are trivially obtained from the above expressions, setting $M_Z=0$.

*On leave of absence from Departament de Física Teòrica, Universitat Autònoma de Barcelona, Bellaterra, Spain.

[1]E. Eichten, I. Hinchliffe, K. Lane, and C. Quigg, Rev. Mod. Phys. **56**, 579 (1984).

[2]For a recent discussion see, e.g., Ref. 1 and G. Altarelli, R. K. Ellis, and G. Martinelli, Z. Phys. C **27**, 617 (1985).

[3]R. Karplus and M. Neuman, Phys. Rev. **80**, 380 (1950); Y. Shima, Phys. Rev. **142**, 944 (1966).

[4]V. Constantini, B. De Tollis, and G. Pistoni, Nuovo Cimento **2A**, 733 (1971).

[5]E. L. Berger, E. Braaten, and R. D. Field, Nucl. Phys. **B239**, 52 (1984); B. L. Combridge, *ibid.* **B174**, 243 (1980); C. Carimalo, M. Crozon, P. Kessler, and J. Parisi, Phys. Lett. **98B**, 105 (1981).

[6](a) R. N. Cahn and J. F. Gunion, Phys. Rev. D **20**, 2253 (1979); (b) M. L. Laursen, M. A. Samuel, G. B. Tupper, and A. Sen, *ibid.* **27**, 196 (1983).

[7](a) M. Glük, E. Hoffmann, and E. Reya, Z. Phys. C **13**, 119 (1982); (b) D. W. Duke and J. F. Owens, Phys. Rev. D **30**, 49 (1984).